Available online at www.sciencedirect.com
SCIENCE DIRECT
Polymer 46 (2005) 2218–2229
polymer
www.elsevier.com/locate/polymer

Changes in the dielectric relaxations of water in epoxy resin as a function of the extent of water ingress in carbon fibre composites

Pascal Boinard[a], William M. Banks[a], Richard A. Pethrick[b,*]

[a]Department of Mechanical Engineering, University of Strathclyde, James Weir Building, 75 Montrose Street, Glasgow G1 1XJ, UK
[b]Department of Pure and Applied Chemistry, University of Strathclyde, Thomas Graham Building, 295 Cathedral Street, Glasgow G1 1XL, UK

Received 7 April 2004; received in revised form 9 November 2004; accepted 10 November 2004
Available online 27 January 2005

Abstract

Dielectric relaxation measurements are reported over a frequency range from 10^{-1} to 10^{9} Hz as a function of exposure time for an epoxy resin–carbon fibre composite, ageing at 60 °C in water. Investigation of the nature of the dipole relaxation of the water molecules, indicates the nature of their interaction with the polymer matrix. Analysis of the dielectric relaxation spectra allow identification of processes that can be attributed to 'free' and 'bonded' water, water in micro-cracking, located in carbon fibre disbonds and plasticizing the polymer matrix. Identification of the various types of location in which water exists was aided by use of the N_g factor from the Kirkwood–Frölich equation, which describes the constraints on free dipole ration nature imposed by the environment in which it is located. These data indicate the power of the dielectric technique for quantitative analysis of water ingress into epoxy composites.

Keywords: Epoxy resin; Water ingress; Dielectric relaxation spectroscopy

1. Introduction

Because of their specific strength, high temperature and chemical resistance and ease of processing, epoxy resins are used for a wide range of applications, including being a major matrix material for carbon fibre composites However, moisture ingress into epoxy resins can have a disadvantageous effect on their mechanical properties. Water penetration in epoxy resins tends to decrease the modulus of the matrix and if it is allowed to segregate, can causes blistering and environmental stress crazing. It has been proposed [1,2] that the transport of moisture below T_g is a three-stage process: (i) diffusion of water through the bulk of the polymer network, (ii) absorption of moisture on the surface of vacuoles that define the excess free volume of the glassy structure and (iii) through hydrogen bond formation between hydrophilic groups associated with hydroxyl or amine groups attached to the polymer chain and the water molecules. The available free volume in the resin [2,3] influences the water equilibrium concentration and can in addition occupy microvoids and other morphological defects [4–7]. A proportion of the water in the microvoids will be bound to hydroxyl and other polar groups which form the surface of the cavity, rather than being in the free-unbound state [4]. Spectroscopic investigation suggests that water molecules, dispersed in the epoxy resin, are linked by strong hydrogen bonds to hydrophilic groups [8,9], mainly hydroxyl [10] or amine groups [11]. When exposed to hygrothermal environments, epoxy composites undergo degradation which manifests itself in terms of reduced structural performance [12–14]. The absorbed moisture is able to facilitate relaxation of the polymer chains leading to changes in the residual stress distribution, plasticisation of the epoxy matrix and the formation of new micro-voids and/or micro-cracks in the resins [15–18]. Some of these degradations or physical ageing processes are closely linked to the swelling processes observed in degraded composite structures. Hahn [19] showed that the absorbed water initially produces relatively little swelling, but once a critical amount of water has been absorbed, subsequent absorption leads to the resin increasing its volume

* Corresponding author. Tel.: +44 141 548 2260; fax: +44 141 548 4822.
E-mail address: r.a.pethrick@strath.ac.uk (R.A. Pethrick).

0032-3861/$ - see front matter © 2004 Elsevier Ltd. All rights reserved.
doi:10.1016/j.polymer.2004.11.103

proportionally to the additional water content absorbed. This critical amount of water may be related to plasticization of the matrix allowing stress relaxation and creation of new micro-void and micro-crack formation.

Over the last few years, the interactions of water with the surrounding polymer have been carefully studied using a diverse range of spectroscopic techniques. However, no definite conclusions have been drawn concerning the precise nature of the interaction of the water molecules with the epoxy resins.

This paper attempts to determine the nature of the relaxation properties of water molecules in an epoxy resins matrix by looking at the dipolar relaxation properties of water using dielectric relaxation spectroscopy (DRS). The dielectric relaxation spectroscopy method, is an extremely effective method of characterising over a very large frequency range, the molecular dynamics of liquids and solids containing mobile polar groupings. The technique is sensitive to orientational motions of permanent dipoles fixed within the material and the translational contribution of ions through the bulk material and within inclusions due to the applied electric field. The DRS method has been extensively used for the characterisation of polymeric materials and in particular for the study of the cure process in thermosets [20–24]. In principle, the DRS technique can provide detailed information on the dipolar activity of the material investigated. In certain systems, ionic conduction may contribute to the electrical properties either as the dc conductivity or polarisation associated with heterogeneities within the resin. Both contributions can give rise to a large dielectric loss and mask the underlying dipole processes. However, in semi rigid solids, these ionic conduction processes are usually suppressed and the dipole relaxation is the main cause of the dominant frequency dependence of the dielectric properties. Water has an exceptionally large dipolar contribution and is ideally suited for investigation of water ingress into the matrix material. Mashimo and co-workers [25–28] spent the last 20 years investigating the dynamics and structure of water in biological materials and polymers in solution. They have successfully identified relaxation processes associated with different states of water which they designate free and bonded. Nowadays, the development of computer controlled network analysers has allowed the determination of dielectric properties in dense materials such as epoxy composites and adhesives [29,30] and allows measurements to effectively be made in real time, allowing investigation of processes which are in a state of dynamic change.

2. Experimental procedure

2.1. Materials

The adherents were manufactured from unidirectional carbon fibre pre-impregnated epoxy film, trade named 914C-TS-5-34 supplied by Hexcel Composites. The pre-impregnated film contains 66% by weight of high tensile Toraya surface treated carbon fibres. The adhesive film used is supported by a polymeric woven film and is a blend of approximately 70% of bis[2-chloro-*N*,*N*-bis(2,3epoxypropyl)-4-aminophenyl]methane and 30% of diglycidylether of bisphenol A which was cured with about 3–7.0% of dicyandiamide and between 0.5 and 1.5% of (*N*,*N*′-(methyl-1,3-phenylen)bis(*N*,*N*′dimethylurea).

2.2. Manufacturing of composite panels

Carbon fibre pre-preg layers were used to produce a series of different lay-up designs using a vacuum bag procedure in an autoclave. Curing was achieved at a temperature of 170 °C under a pressure of 7 bar. A post-cure at 190 °C for 4 h was performed. Joints were manufactured by joining two carbon fibre reinforced plastic (CFRP) plates with a lay-up of adhesive films. The assemblage, placed in an autoclave chamber, was cured using a vacuum bag system at a temperature of 125 °C and a pressure of 2 bar for 1 h. The final system was a single lap joint made of 150 mm length, 50 mm width and 1.8 mm thick CFRP plates bonded over a 10 mm wide overlap by a 1 mm thick adhesive.

2.3. Gravimetric measurements

As soon as they were manufactured, the samples were placed in a dessicator at room temperature in order to avoid absorption of moisture prior to the ageing study. Gravimetric measurements were performed by removing the samples from a water bath held at a constant temperature of 60 °C, rapidly removing excess surface water using tissue paper and weighing using an electronic balance (Mettler AJ100). The measurements were performed with an accuracy of ± 0.1 mg. The samples used for the study were coded, so that it was possible to determine individually the weight difference for each coupon. The time required to carry out the weighing of the coupons was typically less than 2 min which was assumed to be sufficiently short not to influence the values of the mass changes measured. The data are an average for five coupons and the error bars are indicative of the spread of values observed.

2.4. Dielectric measurements

The dielectric measurements were based on two different methods, depending on the frequency range being investigated. At low frequency (0.1 Hz–65 kHz), impedance measurement was used. At high frequency (300 kHz–3 GHz), the method was based on the transmission line principle. Each technique allows determination of the frequency dependence of the dielectric permittivity and dielectric loss of the materials under investigation. Details of the measurements can be found elsewhere [31–33]. The high frequency dielectric measurements were performed

using a computer control network analyser. The frequency sweep was performed, acquired and analysed in less than 30 s. In the case of low frequency measurements, computer control frequency response analyser was used and only five points per decade were acquired minimising the total measurement time to less than 2 min. The measurements of the dielectric properties were conducted at ambient temperature, which was 25 °C in the laboratory. The thickness of the samples were measured using a digital micrometer and the values taken were and average ten points along the length of the coupon. The error bars indicate the mean and maximum variation in the observed values.

The ageing of the samples was carried out at 60 °C in a water bath. In both cases, the time that the sample is out of the ageing bath is sufficiently short for the sample not to have changed and was typically less than five minutes. It is therefore believed that over the time required for the measurements, the state of the water does not vary significantly and the data can be assumed to be a 'snap shot' of the system at the time of measurement. The calculated error in the dielectric data is a combination of the variation in the thickness of the samples and reproducibility errors. Because of the intrinsic conductivity of the carbon fibres the dielectric measurements sample the whole coupon and therefore that data are an average of the effects across the whole sample. The data are an average for the five coupons.

3. Results and discussion

3.1. Water uptake behaviour

The studies were carried out over a period of 5350 h, the specimens spending 2255 h immersed in the 60 °C water bath, followed by a period of 3095 h at 60 °C in an air-circulated oven. Fig. 1 shows the uptake and de-sorption of water as a function of the exposure time to the hot/wet and hot/dry environments. The data in this and subsequent figures are plotted as a function of the root of time. The water absorption by many thermoset materials has been shown to follow a pseudo Fickian type of behaviour and it is therefore appropriate to use this for in plots of the water exposure. Two distinctive features can be identified.

It can be seen that the sorption and desorption processes, do not following the same paths. It is believed that the processes and energy involved for the diffusion of water molecules into the polymeric materials are different from those involved in the desorption process. In the former, the water molecules are adsorbed at the surface of the resin and will fill the surface voids and crazes and then penetrate into the epoxy resin. The energy that is required for the molecules to penetrate the resin will depend on the available volume for their motion. The diffusion process will therefore involve movement of water molecules through the matrix aided by the existence of free volume. Subsequently, further increase in the concentration of absorbed water will require the polymer chains to be separated and this will involve a relatively large amount of energy. Therefore, the rate of sorption decreases as the matrix approaches saturation and is controlled by the capability of the network to rearrange to accommodate the increased number of water molecules. However, the absorbed water can plasticise the polymer matrix, create new free volume and facilitate motion of the polymer matrix allowing stress relaxation with change in the physical dimensions of the polymer. The loss of moisture will lead to a collapse of the matrix back to the structure before it absorbed moisture and this intuitively would be expected to be a reversible process. Other factors can also influence the moisture absorption and desorption. It has been proposed [4,5,18,34] that micro-cracking and disbonding between the

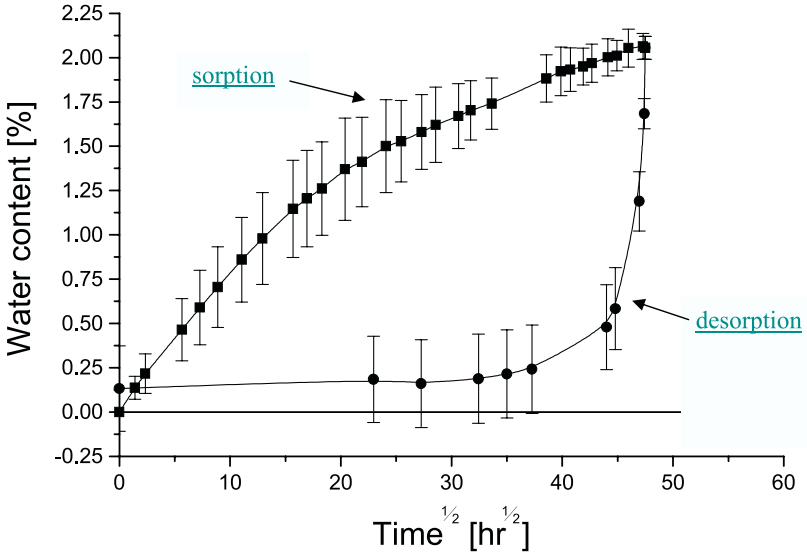

Fig. 1. Water content in the joint structure during (–■–) the sorption and (—●—) desorption process.

matrix and the carbon fibres can occur during the sorption process, mainly due to the non-uniform swelling of the epoxy resins matrix. These newly formed capillary channels, will ease the loss of water molecules during desorption. It is legitimate to assume that during the desorption process, the first molecules to be desorb are those involving the lowest energy. However this type of hysteresis behaviour is similar to the absorption–desorption behaviour of a gas on a surface with 'ink bottle' like pores and therefore consistent with loss of moisture from a channel like cavities. However, highly bonded water molecules associated with the hydroxyl groups of the polymer chain will remain in the resin structure and will need more energy to be displaced from the hydrophilic sites in the networks [35]. This leads to the second observable feature: the water content does not decrease to zero but reaches an equilibrium value of 0.13%. As moisture is lost from the matrix there will be a commensurate loss in the effects of plasticization and the matrix will become more rigid and hence less able to allow moisture transport. Fig. 2 shows the variation of the thickness of the adhesively bonded structure as a function of the water content.

During the first period, i.e. under 225 h of exposure or 1.25% water content, little or no variation occurs. For longer times and greater water uptake there is a steady increase in thickness as a function of time and water content. The first period can be assigned to water molecules permeating the resin matrix and may find and fill micro-voids without changing the overall volume. These water molecules are however forcing the polymer chains apart and induce plasticisation, allowing stress relaxation. Subsequent water absorption, generates swelling of the 3D network resin structure and increases the thickness of the composite. The variation of the thickness during desorption is different from that during the sorption process. The hysteresis effect observed are associated with the emptying of the pore structure created during the absorption process and the subsequent loss of water is from the epoxy matrix material. Therefore, desorption from the bulk, is mainly driven by water transport through the previously formed channels and does not affect the thickness. The water transport from the matrix is steady and contributes to the decrease in the thickness. The overall thickness at the end of the desorption is slightly smaller than the original consistent with a densification of the matrix material. The observed densification is consistent with the resin having been plasticized and being able to move to a thermodynamically more favourable state through relaxation of the stresses frozen in during the fabrication of the coupons.

3.2. Frequency domain analysis

The frequency domain analysis was carried out over nine decades from 0.1 Hz to 100 MHz. Fig. 3(a) and (b) shows the 3D plots of the dielectric permittivity and dielectric loss, respectively, as a function of the exposure time and the frequency. The initial section of the plot is monitoring the water absorption by the coupon. After a time of 2255 h, the samples were then placed in an air oven and the desorption processes monitored. The initial large increases in the dielectric permittivity and loss are observed to be reversed in a similar manner to that observed for the gravimetric measurements, Fig. 1. The changes in the high frequency region of the dielectric spectrum may be attributed to water that is dispersed in the matrix.

The dielectric permittivity and loss show an initial large increase in the low frequency range, below 100 Hz, as exposure time increases. The observed behaviour is a result of a number of effects: (i) a dipolar contribution due to water molecules dispersed in the epoxy resin matrix which is typically observed around the kilohertz region, (ii) shifting of molecular relaxation associated with the hydroxyl groups of the polymeric matrix due to plasticization which is typically observed in the region 1 Hz–1 KHz, (iii) ionic contributions:

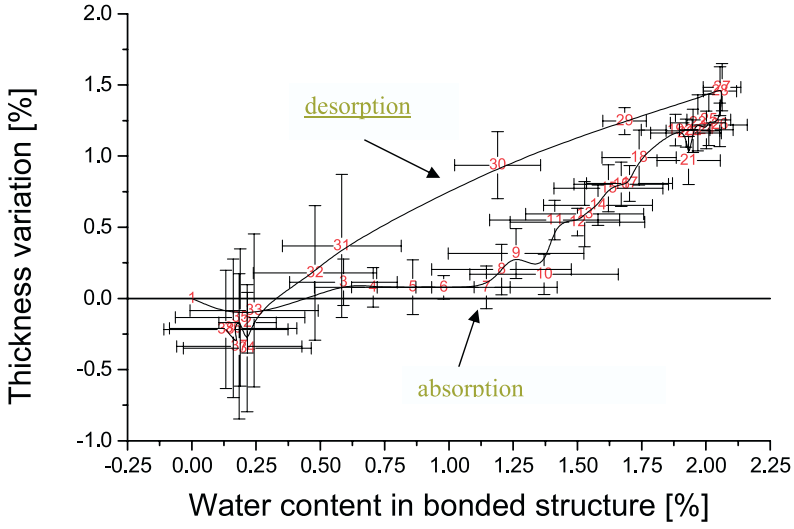

Fig. 2. Evolution of the thickness of the adhesively bonded structure as a function of the water content.

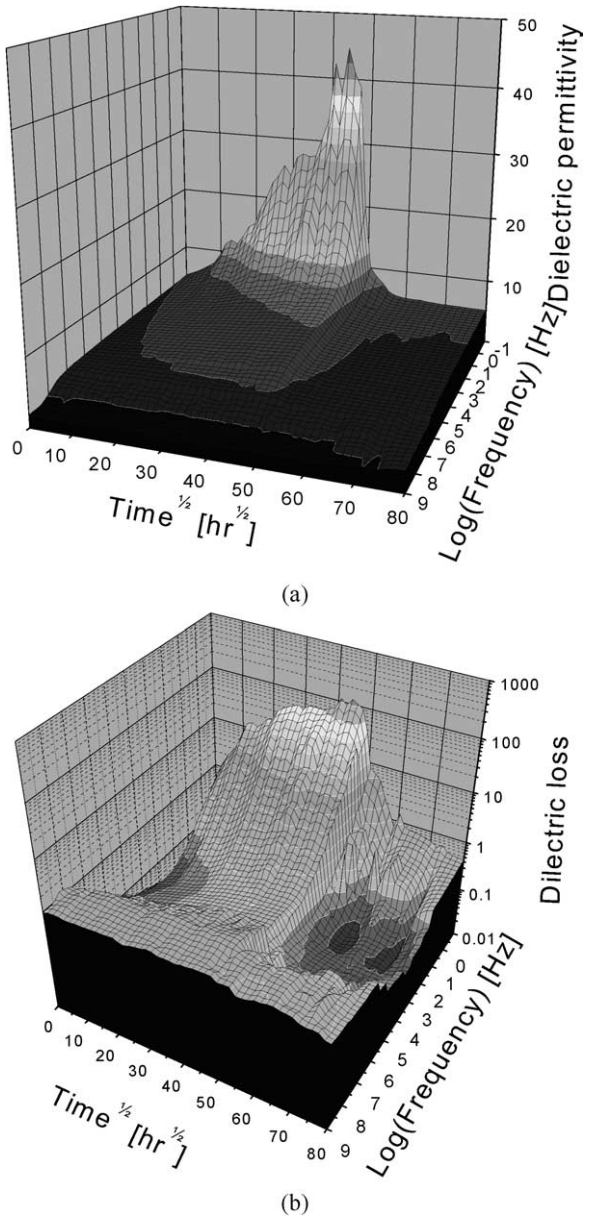

Fig. 3. 3D representation of (a) the dielectric permittivity and (b) the dielectric loss as a function of the frequency and the exposure time to the hot/wet–hot/dry environments.

dc conductivity, MWS and blocking electrodes effects which are typically observed below 10 Hz. The higher frequency contribution above 1 MHz, will also contain contributions due to water which is clustered in voids. In a dicyandiamide cured material, the proportion of hydroxyl groups created will be lower than in an amine cured resin which is reflected in the absence of the usual hydroxyl relaxation process at approximately 10 KHz. The 3D plots of the dielectric characteristics show a sharp decrease of the permittivity and the loss at the start of the desorption process. The original values seem to be recovered after only a few hours of desorption. The high rate of desorption is the result of loss of water in micro voids as well as plasticising the polymer network.

Fig. 4(a) and (b) represents the dielectric permittivity and dielectric loss data, respectively, as a function of the frequency.

As the desorption progresses, it can be seen in Fig. 4(a) that the dielectric permittivity recovers its initial values over the full range of frequency after 1500 h spent in the 60 °C air-circulated oven. The dielectric loss does not recover its initial value in the low frequency range. Moreover, Fig. 4(b) shows a novel feature around 20–30 Hz that can be attributed to a combination of effects. The ingress of moisture will induce morphological changes of the epoxy materials. The swelling of the polymer matrix will plasticise the matrix, allow stress relaxation and stress redistribution. The water can segregate to the fibre–matrix interface and induce dewetting of the fibre by the hydrophilic resin. Disbonding around the fibre may take place in the swollen state, creating new surfaces and these voids can exhibit characteristic relaxation features. It can be seen that the dielectric loss recovers rapidly its value at high frequency that is consistent with the idea that the free water molecules are in voids or channels which are easily accessible to the surface. Hasted [36] demonstrated that water interactions occur mainly through hydrogen bonding. At hydrophobic interface, the water molecules will not be part of an extensive hydrogen bond network and will behave as isolated dipoles. Therefore, different types of dielectric relaxation would be expected. However, a continuous variation of relaxation time of the water dipoles from the interfacial to the bulk material would cause its total loss spectrum to become broad as seen in Fig. 4(b). Moreover, in the case of conductive materials, the dipolar relaxation is embedded in an ionic contribution arising from the formation of an electrical path between the electrodes or MWS processes associated with water filled voids.

To differentiate the dipolar relaxations from the ionic contribution, one has to use the complex electrical modulus formalism [37–39]. In these systems where the low frequency region is a complex mixture of processes it is appropriate to adopt this alternative approach rather than attempting to fit the data with an undetermined number of overlapping processes. The complex electrical modulus

$$M^* = \frac{1}{\varepsilon^*} = M' + iM'' \tag{1}$$

which is defined as the reciprocal of the dielectric constant has most frequently been employed in the investigation of relaxation processes in ionic conductors. To resolve the dipolar and ionic natures of the relaxation processes, the real M' and imaginary M'' components, termed electrical modulus and electrical loss respectively, of the complex electrical modulus M^* can be determined using the following relations

$$M' = \frac{\varepsilon'}{\varepsilon'^2 + \varepsilon''^2} \quad \text{and} \quad M'' = \frac{\varepsilon''}{\varepsilon'^2 + \varepsilon''^2} \tag{2}$$

The data presented in Fig. 4 may be directly substituted

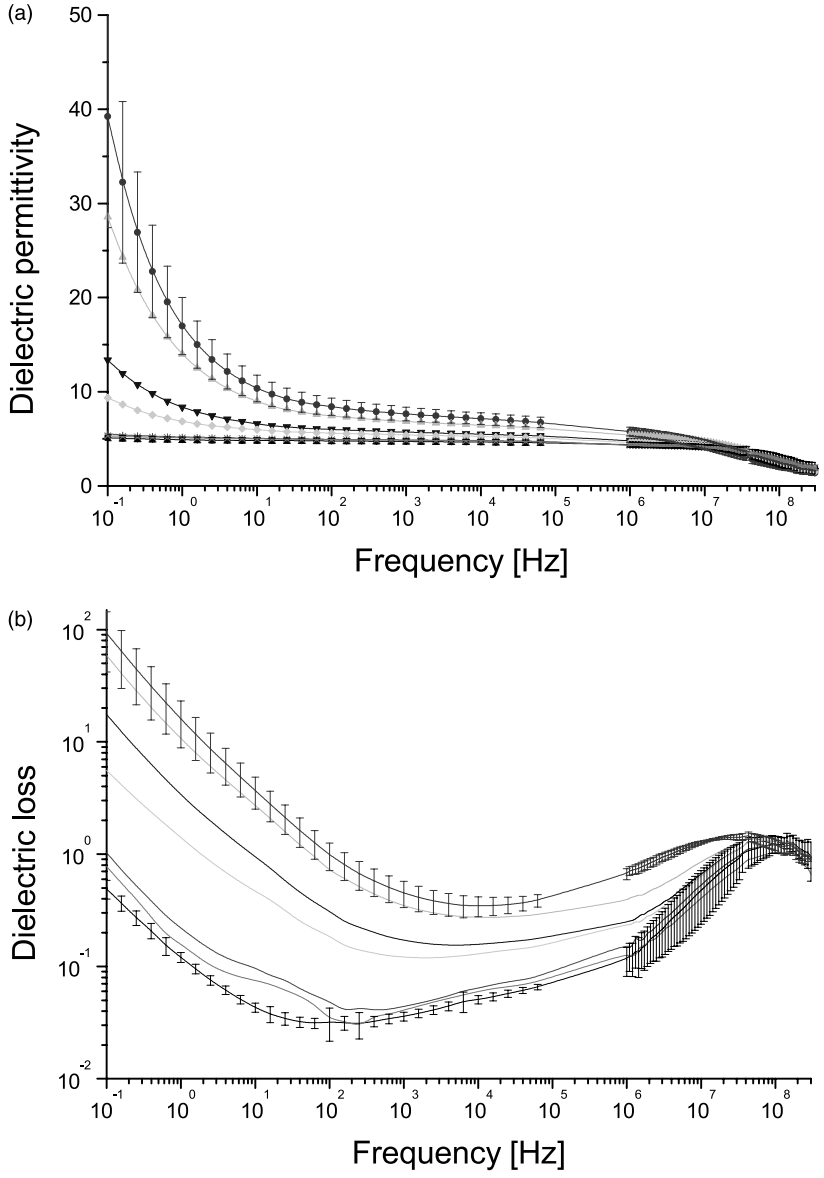

Fig. 4. Dielectric (a) permittivity and (b) loss as a function of the frequency; lowest line is as manufactured, then in ascending order (—) 2 255 hours in the hot/wet environment, followed by (—) 50 hours, (—) 248 hours, (—) 319 hours, (—) 1 512 hours and (—) 3 095 hours in the hot/dry environment.

into Eq. (2), where ε' and ε'' are functions of frequency allowing direct calculation of the respective dielectric modulus M' and M''. Fig. 5(a) and (b) shows the electrical modulus and electrical loss, respectively, as a function of the frequency range during the desorption process.

A large decrease in the electrical modulus can be noticed in Fig. 5(a) at the end of the sorption process. As the water content decreases, the electrical modulus regains its original value. Since the electrical modulus is a representation of the dipolar contribution, it is thought that its depression at the end of the absorption is due to loss of plasticisation as the water is desorbed from the polymeric matrix, the original value is recovered. As shown in Fig. 5(b), the electrical loss presents a feature in the 20 Hz region as well as a limited recovery of its original value.

In order to characterise the different relaxations involved in the sorption and desorption processes, the dielectric characteristics are presented in Cole–Cole plot. Fig. 6 is the Cole–Cole plot representation of the complex electrical modulus.

It shows the recovery of the low frequency value as the water content decreases. The shifting of the relaxation towards lower frequency is a direct consequence of the anti-plasticisation of the polymeric matrix. As the water leaves the inter-chain spaces of the cross-linked network, the distance between the chains decreases and the segments lose mobility consistent with the glass transition temperature [T_g] increasing. Therefore, the dipole contribution disappears. The new loss contribution is confirmed in Fig. 7, which is a close-up of the Cole–Cole representation of the

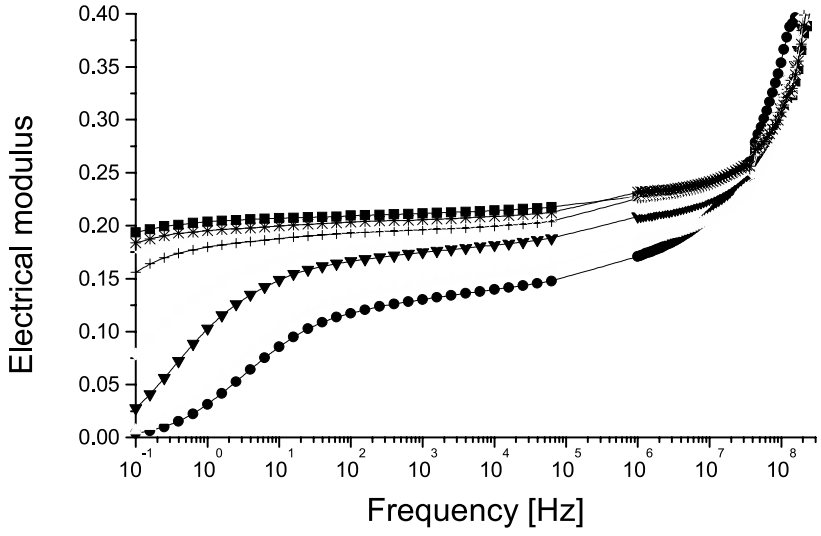

(a)

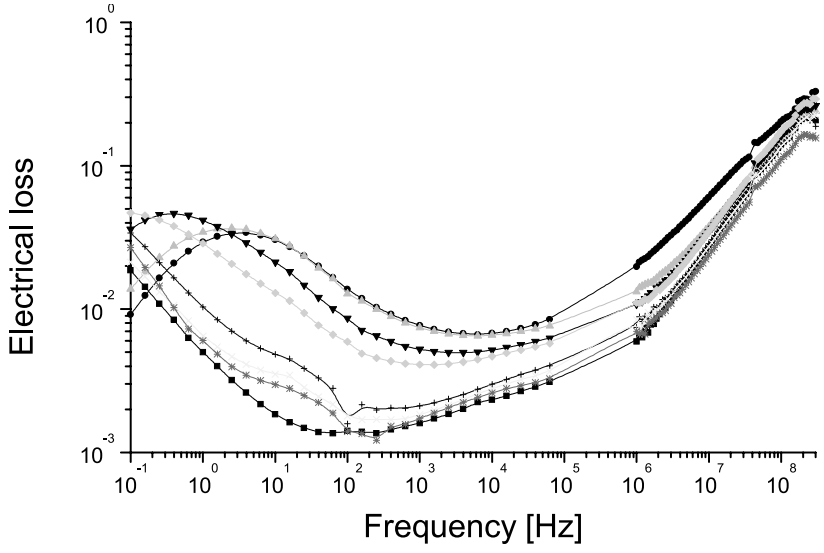

(b)

Fig. 5. Electrical (a) modulus and (b) loss as a function of the frequency during the exposure to the hot/wet and hot/dry environments, (—■—) as manufactured, after (—∗—) 2 255 hours in the hot/wet environment, followed by (—×—) 50 hours, (—+—) 248 hours, (—◇—) 319 hours, (—▼—) 866 hours, (—△—) 1 203 hours and (—●—) 3095 h in the hot/dry environment.

complex electrical modulus in the high range of the low frequency.

To confirm the nature of the dipolar contributions in the low frequency range, dielectric measurements from 0.1 mHz to 65 kHz were performed. Since 24 h are required to gather the data, the experiments were conducted at the end of the dehydration to avoid desorption process during the experiment influencing the data. Fig. 8 presents the electrical modulus and electrical loss over the very low frequency range at the end of the 5350 h investigation period.

The very low frequency gives access to the suspected relaxation. This dielectric process is associated with a combination of dipole and conduction processes associated with the plasticization of the resin enhancing ionic conductivity and modulated by the presence of interfaces within the resin. The low frequency feature is located at approximately 10^{-3} Hz, a weak higher frequency process observed at approximately 10 Hz may be ascribed to the motion of the polymer matrix. The higher frequency process located above 10^5 Hz is ascribed to free water located in voids within the matrix. Mathematical models of dielectric relaxations have been proposed by several authors [36,40,41] depending on the complexity of the medium. The most common representation for dense

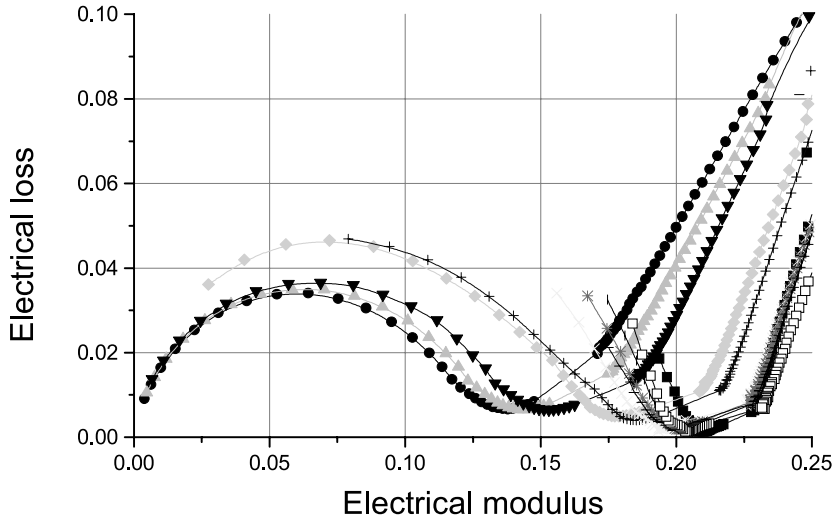

Fig. 6. Cole–Cole plot of the complex electrical modulus during the exposure to the hot/wet and hot/dry environments, (—■—) as manufactured, after (—●—) 2255 hours in the hot/wet environment, followed by (—▲—) 7 hours, (—▼—) 50 hours, (—◆—) 248 hours, (—+—) 319 hours, (—×—) 866 hours, (—∗—) 1030 hours, (— – —) 1203 hours, (—|—) 1512 hours and (—□—) 3095 hours in the hot/dry environment.

cross-linked polymeric network is the Havriliak–Negami equation defined [42,43] as

$$\varepsilon^* = \varepsilon_\infty + \frac{\varepsilon_s - \varepsilon_\infty}{[1 + (j\omega\tau)^\alpha]^\beta} \tag{3}$$

where $0 < \alpha, \beta \leq 1$. For ionic medium, the same formalism can be applied to the complex electrical modulus, which can be described by

$$M^* = M_\infty + \frac{M_{stat} - M_\infty}{[1 + (j\omega T)^a]^b} \tag{4}$$

where M_∞ and M_{stat} are the value of the electrical modulus in the high and low range of the low frequency, respectively. ω is the angular frequency and T is the relaxation time. a and b are the distribution parameters. In a symmetrical relaxation, equivalent to the Cole–Cole situation, the value of b is 1 and at the maximum loss, the following relation exists

$$\omega_{max} T = 2\pi f_{max} T = 1 \tag{5}$$

Eq. (4) can be rewritten as

$$M^* = M_\infty + \frac{M_{stat} - M_\infty}{\left[1 + \left(j\frac{f}{f_{max}}\right)^a\right]^b} \tag{6}$$

where f_{max} is the frequency of the electrical loss maximum. However, most polymeric materials do not present a symmetrical relaxation. The value of b is not equal to 1 and the relation identified at the maximum

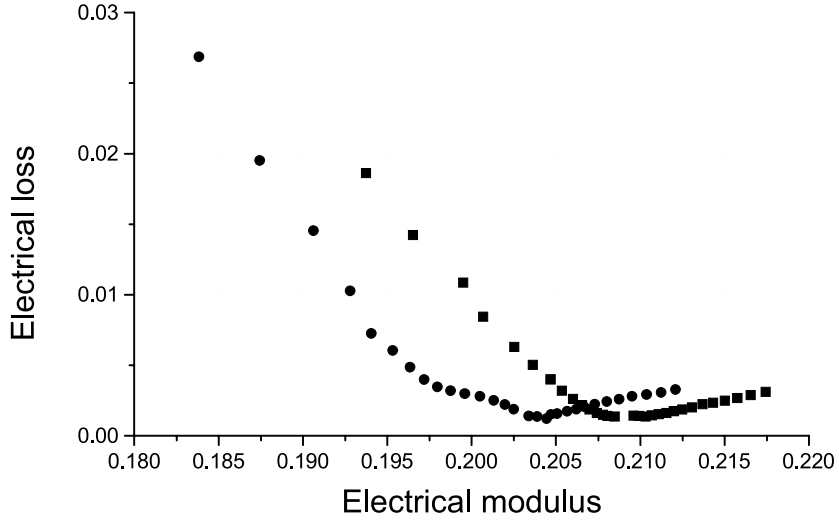

Fig. 7. Cole–Cole plot of the complex electrical modulus of (■) the unaged structure and (●) the structure after 2255 h hydration and 3095 h dehydration cycling.

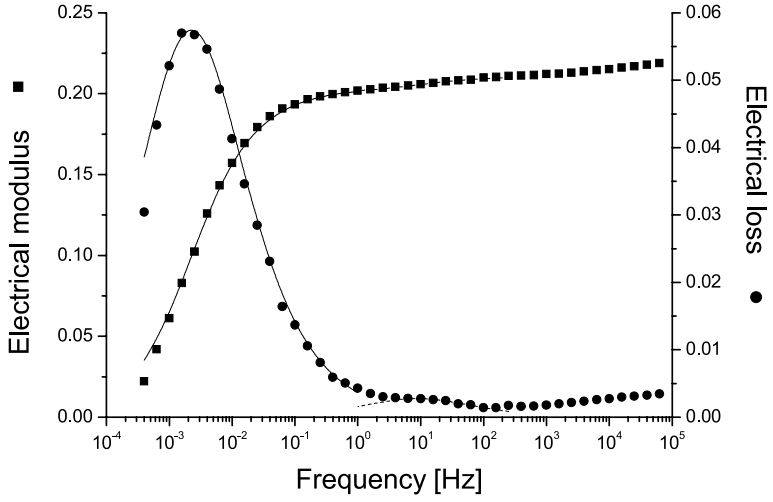

Fig. 8. The symbols represent the experimental data points for the electrical modulus (■) and loss (•) and the lines are the theoretical electrical modulus and electrical loss as a function of the frequency range.

loss has to be modified as follow [44–46]

$$\omega_{\max}\tau = \left[\frac{\sin\left(\frac{\pi ab}{2(1+b)}\right)}{\sin\left(\frac{\pi a}{2(1+b)}\right)}\right]^{1/a} = \Gamma \tag{7}$$

Therefore, Eq. (6) becomes

$$M^* = M_\infty + \frac{M_{\text{stat}} - M_\infty}{\left[1 + \left(j\frac{f\Gamma}{f_{\max}}\right)^a\right]^b} \tag{8}$$

The solid lines in Fig. 8 are the best fit of data in the very low frequency relaxation using Eq. (8) with $M_\infty = 0.204$, $M_{\text{stat}} = 0$, $f_{\max} = 0.0017$ Hz, $\alpha = 0.68$ and $\beta = 0.9$, giving $\Gamma = 0.91$. The dash lines are the best fit for the second relaxation with $M_\infty = 0.2105$, $M_{\text{stat}} = 0.2005$, $f_{\max} = 9$ Hz, $\alpha = 0.65$ and $\beta = 1$, giving $\Gamma = 1$. Fig. 9 presents the Cole–Cole plot of the complex electrical modulus. The limiting values in the above equation are obtained from the iterative fitting of Eq. (8) to the experimental data. It shows the various dipolar relaxations obtained experimentally and mathematically.

The first relaxation is obtained with values of a and b less than 1. It signifies that the relaxation is not defined as a pure Debye relaxation for which case a single relaxation process is defined. Therefore, it is believed that this relaxation is a combination of dipolar contributions. The second relaxation is obtained with values of a less than 1 and b equal to 1. This is the definition of the Cole–Cole equation for which the relaxation is centred on the frequency of the electrical loss maximum, indicating a single relaxation time for the process.

The Kirkwood–Frölich equation [47,48] indicates that the dielectric permittivity ε_s of a material is directly related to the number of dipoles per unit volume N present in that material

$$\frac{(\varepsilon_S - \varepsilon_\infty)(2\varepsilon_S + \varepsilon_\infty)}{\varepsilon_S(\varepsilon_\infty + 2)^2} = \frac{4\pi\mu_0^2}{9kT}Ng \tag{9}$$

where ε_∞ is the dielectric permittivity at very high frequency which in this system can be equated to the dry resin value and is a constant, g is the orientation correlation function and is a measure of the constraints imposed on the free relaxation induced by the local ordering in the material, k is Planck's constant, T is the temperature and μ_0 is the dipole moment of the molecule. Hill et al. [49], based on the work of Kirkwood and Frölich, calculated the values of ε_∞ and μ_0 for water molecule as 4.55 and 1.84 D (D being the Debye unit $= 10^{-18}$ e.s.u. $= 10^{-18}$ statcoulomb cm), respectively. Therefore water uptake could be assessed by assuming that the variation in the dielectric permittivity of a material during exposure to water is caused by a variation in the number of dipoles present, mainly water dipoles [40].

It has to be emphasised that in the present studied system, water dipoles are not the only source of dipoles inside the structure, but being a dicyandiamide cured system the number of hydroxyl groups will be relatively low in comparison to the typical amine cured system. Proof of this assumption is the finite value of the Ng factor at time zero. However, it is assumed that from this dry state, the only source of new dipoles come from the ingress of water molecules inside the epoxy resin. Fig. 10 shows the evolution of the Ng factor as a function of the water content in the adhesively bonded structure.

The error bars are an indication of the uncertainties introduced by the various uncertainties in the original data and the transformations subsequently carried out to obtain the parameter. As the water molecules penetrate the bonded structure, they firstly fill the voids and crazes present in the epoxy matrix. In terms of dipole and dipolar interactions, this means that water molecules are transported through the materials with little or no interaction with the surrounding polymer or other penetrant molecules. This gives rise to the first linear section of the curve up to 1.25% water content, showing a simple augmentation of the number of dipoles (N). As the water content increases further, the water

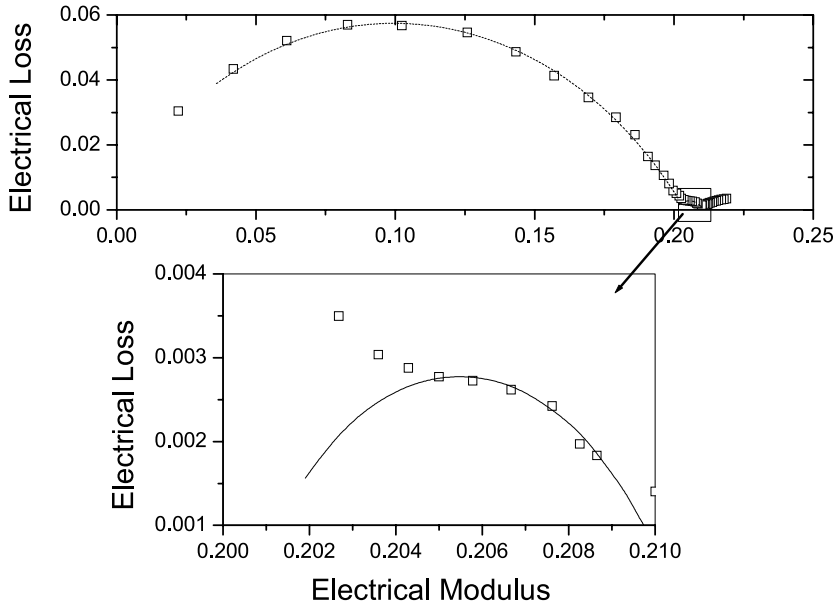

Fig. 9. Cole–Cole plot of the complex electrical modulus, (□) experimental data and theoretical (- - -) very low and (—) low frequency relaxations.

molecules enter the cross-linked network of the epoxy resins. At this stage, the *Ng* factor is influenced not only by the increase of the number of dipoles, *N*, but also by the interactions that those molecules have with the surrounding medium and with each other lead to an increase in *g*. This is exhibited by the second linear region. During the desorption process, the variation of the *Ng* factor does not follow the sorption path. This hysteresis phenomenon is linked to the different processes involved during the hydration and dehydration of the structure.

During the desorption process, the first molecules to depart from the polymeric materials are those having little interactions with their surrounding leading to a decrease of *N* but little change in *g*. This feature is shown by a first approximately linear variation from 2.1 to 1.1% water content. After this water molecules having a higher dipolar interaction, such as those having plasticised the cross-linked network of the epoxy, desorb and a larger decrease in the *Ng* factor can be noticed from around 1.1% to the final value of the dehydration experiment. The four successive stages of the absorption and desorption process are depicted in Fig. 11.

Under 1.25% water content, the water fills the micro and macro-voids. No drastic changes are noticed in the thickness of the structure. The filler in the diagram is the carbon fibre. Above 1.25% water content, transport of water from the

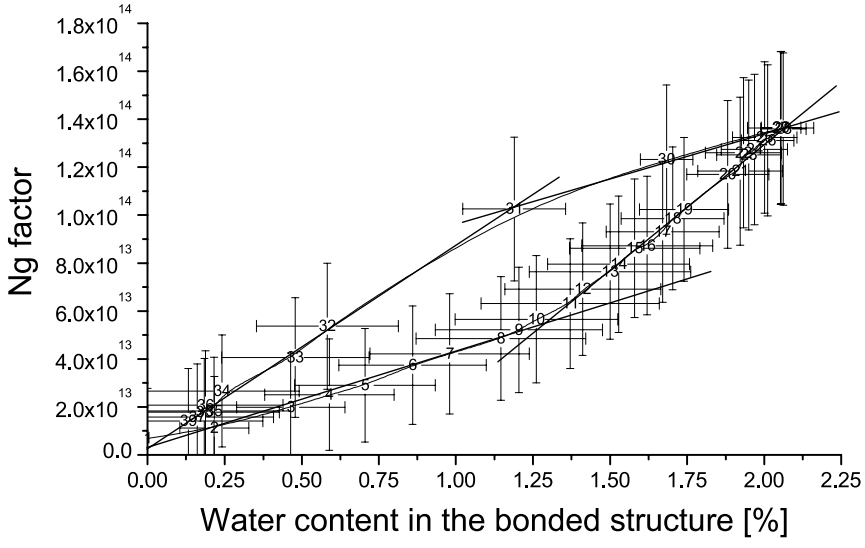

Fig. 10. Evolution of the *Ng* factor as a function of the water content in the adhesively bonded structure.

filled voids towards the bulk of the material happens with water molecules penetrating the cross-linked network and swelling takes place. At the same time, development of micro-cracks and interface disbonding occurs, increasing the water content and the thickness of the structure. During the desorption process, the water molecules unbonded to the medium desorb rapidly through capillary paths generated during the sorption process, followed by the exchange between the wet matrix and the 'dry' voids, yielding to the decrease of the thickness due to matrix 'de-swelling'.

4. Conclusion

During the different environmental ageing stages of carbon fibre composite structures, the frequency domain analysis has been able to show various types of dipolar activities, as well as conductivity contributions, known as Maxwell–Wagner–Sillars (MWS) and blocking electrode effects The main contributions observed at low frequency are linked to the conductivity contributions and the presence of water in the epoxy resin matrix. The latter type of water, termed bonded water, acts on two levels. It produces a large ionic contribution by diluting and by redistributing mobile charges into the adhesive layer. It also plasticises the epoxy matrix and a depression in the dipolar relaxation-ionic conductivity is observed at very low frequency. To resolve the different contributions, it was demonstrated that the complex electrical modulus formalism allows additional information to be obtained by minimising the effect of the conductivity term. By this means, two main relaxations were observed. The first one, is related to the second order relaxation process of the adhesive, termed β-relaxation. This relaxation is significantly altered by the presence of water. A shifting towards higher frequency due to higher chain mobility has been observed as the water is absorbed. It is a confirmation of the plasticisation of the epoxy resin.

A second relaxation appears at a higher frequency, during the sorption–desorption cycling procedure and could be clearly seen in dehydrated samples. One or a combination of the following two processes could be responsible for this relaxation. Firstly, it could be related to the redistribution of the ionic charges towards the adhesive–adherent interfaces. As water penetrates the adhesive, ionic impurities left over from the epoxy resin synthesis will become hydrated and add to the transport mechanism and be influenced by the electrical field. Secondly, this relaxation could also be related to new polymeric chain entities free to rotate at the newly formed free surfaces generated by microcracking and disbonding around fillers and reinforcement. The frequency domain analysis allowed the interpretation of the water transport into the adhesive material and a proposition was made concerning the path that water might take during the ageing processes. Using the Kirkwood analysis it is possible to gain further insight into the nature of the processes being studied. The *Ng* factor takes into account the number of dipoles present in a unit volume as well as their interaction with the surrounding matrix. It has been shown that during hydration–dehydration experiments, four steps are necessary for the water to penetrate and to desorb the adhesive. These four steps have been identified relative to gravimetric and dielectric analysis. The different interactions that water has with the polymeric medium result in different rates of transport, which can be identified in the *Ng* factor behaviour by a hysteresis phenomenon.

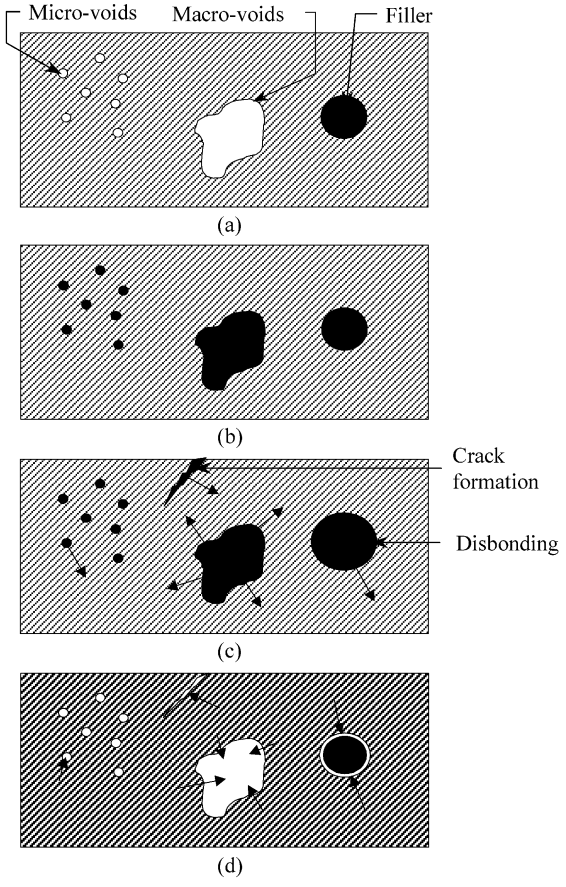

Fig. 11. Schematic representation of water transport in the polymeric materials, (a) dry material, (b) sorption period from 0 to 1.25% water content: the water fill the voids, no swelling occurs, (c) sorption period over 1.25%: the water penetrates the 3D network, swelling, micro-cracking and disbonding around the fillers occur and (d) desorption period: first the water transport occurs from voids and cracks, then water is desorbed from the cross-linked network and de-swelling takes place.

Acknowledgements

One of the authors (P.B.) wishes to thank the Non Destructive Evaluation Branch, Materials Directorate of the US Air Force for the provision of a maintenance grant in support of this study (grant No. F49620/97/1/0350), British

Aerospace for the provision of materials, and Dr D. Hayward of the Department of Pure and Applied Chemistry, University of Strathclyde, for his high frequency dielectric spectroscopy knowledge and advice.

References

[1] Apicella A, Nicolais L, de Cataldis C. In: Kaush HH, Zachman HGZ, editors. Advances in polymer science, vol. 66. Berlin: Springer; 1985. p. 189–207.
[2] Adamson MJ. J Mater Sci 1980;15:1736–45.
[3] Enns JB, Gilham JK. J Appl Polym Sci 1983;28:2831–46.
[4] Diamant Y, Marom G, Broutman LJ. J Appl Polym Sci 1981;26: 3015–25.
[5] Gupta VB, Drzal LT, Rich MJ. J Appl Polym Sci 1985;30:4467–93.
[6] Soles CL, Chang FT, Gidley DW, Yee AF. J Polym Sci Part B: Polym Phys 2000;38:776–91.
[7] Soles CL, Yee AF. J Polym Sci Part B: Polym Phys 2000;38:792–802.
[8] Jelinski LW, Dumais JJ, Stark RE, Ellis TS, Karasz FE. Macromolecules 1983;16:1019–21.
[9] Jelinski LW, Dumais JJ, Cholli AJ, Ellis TS, Karasz FE. Macromolecules 1985;18:1091–5.
[10] Danieley ND, Long RE. J Polym Sci—Polym Chem Ed 1981;19: 2443–9.
[11] Carfagna C, Apicella A, Nicolais L. J Appl Polym Sci 1982;27: 105–12.
[12] Thomas DK. In: Bloor D, Brook RJ, Flemmings MC, Mahajan S, editors. The encyclopedia of advanced materials, vol. 1. Oxford: Elsevier; 1994. p. 55–62.
[13] De'Nève B, Shanahan MER. Polymer 1993;34(24):5099–205.
[14] Xiao GZ, Shanahan MER. J Polym Sci, Part B: Polym Phys 1997; 35(16):2659–70.
[15] Wright WW. Composites 1981;201–4.
[16] Apicella A, Nicolais L, Astarita G, Dorioli E. Polymer 1979;20: 1143–8.
[17] Morgan RJ, Mones ET. In: May C, editor. Resins in aerospace. ACS symposium series, vol. 132. Washington: American Chemical Society; 1980. p. 233–45.
[18] Lee MC, Peppas NA. Prog Polym Sci 1993;18:947–61.
[19] Hahn HT. J Compos Mater 1976;10:266–78.
[20] Senturia SD, Sheppard NF. Dielectric analysis of thermoset cure. In: Dusek K, editor. Epoxy resins and composites IV. Berlin: Spinger; 1986.
[21] Wetton RE, Foster GM, Gearing JWE, Richmond JC. Dielectric cure studies for composites. In: Saporiti F, Merati W, Peroni L, editors. New generation materials and processes. Milano: Grafiche FBM; 1988. p. 329–37.
[22] Tabellout M, Randrianantoandro H, Emery JR, Durrand D, Hayward D, Pethrick RA. Polymer 1995;36(24):4547–52.
[23] Fitz BD, Mijovic J. Polym Adv Technol 1998;9(10-11):721–6.
[24] Johari GP, Ferrari C, Salvetti G, Tombari E. Phys Chem—Chem Phys 1999;1(12):2997–3005.
[25] Mashimo S, Kuwabara S, Yagihara S, Higasi K. J Phys Chem 1987; 91:6337–8.
[26] Mashimo S, Miura N. J Phys Chem 1993;99(12):9874–81.
[27] Shinyashiki N, Matsumara Y, Miura N, Yagihara S, Mashimo S. J Phys Chem 1994;98:13612–5.
[28] Naito S, Hoshi M, Mashimo S. Anal Biochem 1997;251:163–72.
[29] Banks WM, Hayward D, Joshi SB, Li Z-C, Jeffrey K, Pethrick RA. Insight 1995;37(12):964–8.
[30] Affrossman S, Banks WM, Hayward D, Pethrick RA. Proc Inst Mech Engl 2000;214:87–102.
[31] Li Z-C, Joshi SB, Hayward D, Gilmore R, Pethrick RA. NDT E Int 1997;30(3):151–61.
[32] Boinard P, Boinard E, Pethrick RA, Banks WM, Crane RL. Sci Eng Compos Mater 1999;8(4):175–9.
[33] Boinard P, Pethrick RA, Banks WM, Crane RL. Insight 2001;43(3): 159–62.
[34] Chateauminois A, Vincent L, Chabert B, Soulier JP. Polymer 1994; 35(22):4766–74.
[35] Xiao GZ, Shanahan MER. Polymer 1998;39(14):3253–60.
[36] Hasted JB. Aqueous dielectrics. London: Chapman and Hall; 1973.
[37] Parthun MG, Johari GP. J Chem Soc—Faraday Trans 1995;91(2): 329–35.
[38] Migahed MD, Bakr NA, Abdel-Hamid MI, El-Hanafy O, El-Nimr M. J Appl Polym Sci 1996;59:655–62.
[39] Roling B. J Non-Crystal Solids 1999;244:34–43.
[40] McCrum NG, Read BE, Williams G. Anelastic and dielectric effects in polymeric solids. London: Wiley; 1967.
[41] Cole RH. In: Goodman CHL, editor. Physics of dielectric solids. The Institute of Physics Conference Series No. 58.
[42] Havriliak S, Negami S. J Polym Sci-Part C: Polym Symp 1966;14: 99–117.
[43] Havriliak S, Negami S. Polymer 1967;8:161–210.
[44] Díaz-Calleja R. Macromolecules 2000;33:8924.
[45] Schröter K, Unger R, Reissig S, Garwe F, Kahle S, Beiner M, Donth E. Macromolecules 1998;31:8966–72.
[46] Boersma A, Van Turnhout J, Wubbenhorst M. Macromolcules 1998; 31:7453–60.
[47] Kirkwood JG. J Chem Phys 1939;7.
[48] Fröhlich H. Theory of dielectrics. London: Oxford University Press; 1949.
[49] Hill NE, Vaughan WE, Price AH, Davies M. Theoretical treatment of permittivity and loss. In: Sugden TM, editor. Dielectric properties and molecular behaviour. London: Van Nostrand Reinhold; 1969. p. 1–107.